Data-driven fixed-structure frequency-based $\mathscr{H}_2$ and $\mathscr{H}_\infty$ controller design

Philippe Schuchert, Vaibhav Gupta, Alireza Karimi

Laboratoire d'Automatique, École Polytechinique Fédérale de Lausanne (EPFL), Switzerland

Abstract

The frequency response data of a system is used to design fixed-structure controllers for the $\mathscr{H}_2$ and $\mathscr{H}_\infty$ synthesis problem. The minimization of the two and infinity norm of the transfer function between the exogenous inputs and performance outputs is approximated by a convex optimization problem involving Linear Matrix Inequalities (LMIs). A very general controller parametrization is used for continuous and discrete-time controllers with a matrix transfer function or state-space representation. Numerical results indicate that the proposed data-driven method gives equivalent performance to model-based approaches when a parametric model is available.

Key words: Data-driven control; Linear multivariable systems; Linear matrix inequalities; Robust controller synthesis; Convex optimization.

1 Introduction

With recent advancements in computational power and sensor technologies, data-driven control approaches are becoming valuable alternatives to the classical model-based control approach. These methods are extremely useful in situations where system models are either unavailable or involve considerable uncertainties. The methods under consideration usually minimize a control criterion given as a function of the measured data, thus no parametric plant model is needed. The measurement noise is the only significant source of uncertainty, which can be significantly reduced by optimizing over a large enough measurement data set. It can be shown that direct data-driven control can outperform two-step methods where a model is identified in the first step, and a model-based design is used in the second step [8].

Data-driven methods use either time-domain or frequency-domain data. In this paper, the frequency response data, which can be directly obtained from a Fourier Transform of the time-domain data, is used to design a controller. The frequency response function (FRF) and its use for controller design have a well-established place in control. In classical loop-shaping methods, it is used to compute (often manually) simple lead-lag or PID controllers for SISO stable plants and, in Quantitative Feedback Theory (QFT), to compute robust controllers. More recent techniques using only the FRFs have renewed the interest in such techniques. In [14], the set of all stabilizing PID controllers with $\mathscr{H}_\infty$ performance is obtained using only frequency-domain data. In [19], a convex-concave optimization algorithm is used to design robust PID controllers in the QFT framework. In [9,24], the use of the FRF for computing SISO-PID controllers by convex optimization is proposed. These methods use the same type of linearization of the constraints as in [11]. In [6], an extension of the method in [9] for the design of MIMO-PID controllers by linearization of quadratic matrix inequalities is proposed. A similar approach, with the same type of linearization, is used in [25] for designing linearly parameterized MIMO controllers (including PID controllers as a special case). In [2], a non-smooth optimization technique is used to compute fixed structure $\mathscr{H}_\infty$ controllers for infinite dimensional systems (represented by their FRFs). In [13], a frequency-based data-driven control design methodology with $\mathscr{H}_\infty$ control objective based on coprime factorization of the controller is proposed and applied to the current controllers in power converters for particle trajectory control in CERN's accelerators [20,21], control of a hard disk [4] and a multi-actuator drive [26]. An extension of this method to linear parameter-varying MIMO systems is given in [5]. Finally, a fixed-structure data-driven con-

[1] This work is funded by INNOSUISSE 48289.1 IP-ENG and Swiss National Science Foundation under the grant No.200021-204962.

[2] Corresponding author: Alireza Karimi

troller design method for multivariable systems with mixed $\mathscr{H}_2/\mathscr{H}_\infty$ sensitivity performance is proposed in [12] and applied to the distributed control of microgrids [18] and Atomic Force Microscopes [10,22].

In this paper, a solution for generalized systems is developed for the design of a fixed-structure controller using only the FRFs. $\mathscr{H}_2$ and $\mathscr{H}_\infty$ control problems are solved by convex optimization algorithms for continuous and discrete-time systems. The contributions of the paper can be summarized as follows: (1) Design of fixed structured (e.g., centralized, decentralized, and distributed) controllers for closed-loop systems described by a Linear Fractional Representation (LFR). (2) Introduction of new controller structures: both right and left factorizations, enabling more flexible parameterization for non-square controllers. (3) Design of state-space controllers (fixed-order controllers) with improved numerical scaling. (4) Development of a new stability theorem with less restrictive assumptions compared to [12], applicable to both continuous-time and discrete-time systems.

The rest of the paper is organized as follows: preliminaries and the description of the problem are given in Section 2. The main results are developed in Section 3 and several controller parameterizations are proposed in Section 4. Implementation considerations are discussed in Section 5. Numerical examples and comparisons are presented in Section 6. Experimental results are given in Section 7 and concluding remarks in Section 8.

2 Preliminaries

Notation: The set of real numbers is denoted $\mathbb{R}$ and the set of complex numbers $\mathbb{C}$. The set of real rational stable transfer functions with bounded infinity norm is denoted by $\mathscr{RH}_\infty$. $M \succ (\succeq)\, N$ indicates that $M - N$ is a positive (semi) definite matrix, and $M \prec (\preceq)\, N$ indicates $M - N$ is negative (semi) definite. The zero and identity matrix of appropriate size is denoted $\mathbf{0}$ and, I respectively. The conjugate transpose of a complex matrix M is denoted by M^*. The conjugate transpose of the diagonally opposed element in a square matrix is denoted $\star$. If $M \in \mathbb{C}^{n\times m}$ has full row rank, its right inverse is defined as $M^{\mathsf{R}} := M^*(MM^*)^{-1}$. It is clear that $MM^{\mathsf{R}} = I$ and $M^{\mathsf{R}}M$ are Hermitian. If M is full column rank, then its left inverse is defined as $M^{\mathsf{L}} := (M^*M)^{-1}M^*$. Then, $M^{\mathsf{L}}M = I$, and MM^{L} is Hermitian. If M is square and full rank, then $M^{\mathsf{R}} = M^{\mathsf{L}} = M^{-1}$.

2.1 Problem description

A generalized Linear Time-Invariant (LTI) system, mapping exogenous disturbances $w \in \mathbb{R}^{n_w}$ and control inputs $u \in \mathbb{R}^{n_u}$ to performance channels $z \in \mathbb{R}^{n_z}$ and measurements $y \in \mathbb{R}^{n_y}$ is given as follows:

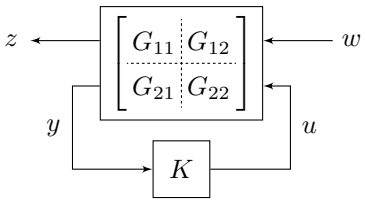

Fig. 1. Lower fractional transform interconnection of system and controller

$$z = G_{11}w + G_{12}u \tag{1a}$$
$$y = G_{21}w + G_{22}u \tag{1b}$$

We assume that only the FRF of the generalized system

$$G(j\omega) = \left[\begin{array}{c:c} G_{11}(j\omega) & G_{12}(j\omega) \\ \hdashline G_{21}(j\omega) & G_{22}(j\omega) \end{array}\right] \tag{2}$$

is available, where $G_{ij}(j\omega)$ are FRFs of appropriate size. The frequency response of the (discrete-time) plant $G_{22} = -P$ can be estimated using the Fourier analysis method from n_u sets of finite input/output sampled data as [23]:

$$P(e^{j\omega}) = \left[\sum_{k=0}^{N-1} \mathbb{Y}(k)e^{-j\omega T_s k}\right]\left[\sum_{k=0}^{N-1} \mathbb{U}(k)e^{-j\omega T_s k}\right]^{-1} \tag{3}$$

where N is the number of data points for each experiment and T_s is the sampling period. The FRF of $P(e^{j\omega})$ can be computed $\forall\omega \in [0, \pi/T_s)$ using (3). Each column of $\mathbb{U}(k)$ and $\mathbb{Y}(k)$ represents respectively the inputs and the outputs at sample k from one experiment, and n_u different experiments are needed to extract $P(e^{j\omega})$ from data. It is assumed that the input signal is persistently exciting, and the synthesis process takes into account the estimation errors caused by truncation and noise in the plant's frequency response.

The synthesis objective is to design a fixed-structure feedback controller K that regulates the effect of the exogenous disturbances w onto the performance channels z. The corresponding block-diagram, shown in Figure 1, is commonly referred to as a lower fractional transformation (LFT) and is given by

$$\mathscr{F}_l(G, K) = G_{11} + G_{12}K(I - G_{22}K)^{-1}G_{21}. \tag{4}$$

The controller is assumed to be part of a set of structured controllers $\mathscr{K}$ that will be detailed in Section 4.

This paper will focus on both $\mathscr{H}_2$ and $\mathscr{H}_\infty$ norm of $T_{zw} = \mathscr{F}_l(G, K)$. In contrast to the standard literature on $\mathscr{H}_2$ or $\mathscr{H}_\infty$, it is not necessary to have knowledge of

a state-space representation of G; only its FRF is required. Under the assumption that the closed-loop system is stable, the norm of T_{zw} can be expressed using only its FRF:

$$\|T_{zw}\|_2^2 = \frac{1}{2\pi}\int_\Omega \operatorname{trace}\left(T_{zw}(j\omega)T_{zw}^*(j\omega)\right)d\omega \quad (5a)$$

$$\|T_{zw}\|_\infty^2 = \sup_{\omega\in\Omega}\ \overline{\sigma}\left(T_{zw}(j\omega)T_{zw}^*(j\omega)\right) \quad (5b)$$

where $\overline{\sigma}(\cdot)$ is the maximum singular value and Ω the frequency spectrum. For continuous-time (CT) systems, Ω is given by $\Omega := \mathbb{R}\cup\{\infty\}$ and for discrete-time systems (DT) by $\Omega := [-\pi/T_s, \pi/T_s)$. $G(j\omega)$ will be used to denote the frequency response of G in both cases.

The controller design problem can be formulated as the minimization of an upper bound on the system norms

$$\begin{aligned} &\min_{K\in\mathscr{K},\,\Gamma}\ \gamma \\ \text{subject to}: \ &K \text{ stabilizes the closed-loop} \\ &T_{zw}(j\omega)T_{zw}^*(j\omega)\preceq\Gamma(j\omega),\quad \forall\omega\in\Omega \end{aligned} \quad (6)$$

where $\Gamma(j\omega)$ is a Hermitian matrix. For the $\mathscr{H}_\infty$ norm, $\Gamma(j\omega)=\gamma I$, where $\gamma\in\mathbb{R}$ and for the $\mathscr{H}_2$ norm, we have:

$$\gamma = \frac{1}{2\pi}\int_\Omega \operatorname{trace}\left(\Gamma(j\omega)\right)d\omega \quad (7)$$

3 Developments

The following assumptions will be made for the generalized plant model:

- (A1) One of the following is true
  - (A1.a) $G_{21}(j\omega)$ has full row rank $\forall\omega\in\Omega$.
  - (A1.b) $G_{12}(j\omega)$ has full column rank $\forall\omega\in\Omega$.
- (A2) $G(j\omega)$ is bounded for all $\omega\in\Omega$.

Remark: (A1) is related to the control performance specifications, and similar equivalent assumptions exist on the rank of some matrices in the state-space model-based approaches [28]. (A1.a) is made to ensure that any possible disturbances have an effect on the measurements. Such a situation, from a control design perspective, indicates that either more sensors or better placement is required for the desired objective. Similarly, (A1.b) ensures that any possible control input has an effect on the performance channels, and its relaxation indicates the need for a better selection of performance channels.

In this paper, right or left factorization (RF or LF) of the controller K is considered as $K=XY^{-1}$ or $K=Y^{-1}X$, where $X\in\mathscr{X}\subset\mathscr{RH}_\infty$ and $Y\in\mathscr{Y}\subset\mathscr{RH}_\infty$. $\mathscr{X}$ and $\mathscr{Y}$ are parametrizations, linear in the optimization variables and should be chosen such that XY^{-1} for the RF, or $Y^{-1}X$ for the LF, reflects the choice of the desired structure in $\mathscr{K}$. Examples of controller structures are given in Section 4.

3.1 Right factorization of the controller

Assume that G_{21} has full row rank and the controller $K=XY^{-1}$ is right factorized (RF).

Then, the transfer function T_{zw} can be rewritten as

$$T_{zw} = G_{11} + G_{12}X\left(Y - G_{22}X\right)^{-1}G_{21} \quad (8)$$

Since G_{21} has full row rank, its right inverse G_{21}^{R} exists, and we can define

$$\Phi = G_{21}^{\mathsf{R}}\left(Y - G_{22}X\right) \quad (9)$$

which is linear in controller parameters. If Φ has full column rank, i.e., the feedback interconnection is well-posed, its left inverse Φ^{L} is given by $\left(Y-G_{22}X\right)^{-1}G_{21}$. Denoting $\Psi = I - \Phi\Phi^{\mathsf{L}} = I - G_{21}^{\mathsf{R}}G_{21}$, then the closed-loop transfer function can be written as

$$\begin{aligned} T_{zw} &= G_{11} + G_{12}X\Phi^{\mathsf{L}} = G_{11}(\Phi\Phi^{\mathsf{L}}+\Psi) + G_{12}X\Phi^{\mathsf{L}} \\ &= \left(G_{11}\Phi + G_{12}X\right)\Phi^{\mathsf{L}} + G_{11}\Psi \end{aligned} \quad (10)$$

The inequality in (6) can then be reformulated as

$$\begin{aligned} T_{zw}T_{zw}^* = &\left(G_{11}\Phi + G_{12}X\right)\left(\Phi^*\Phi\right)^{\mathsf{L}}\left(G_{11}\Phi + G_{12}X\right)^* + \\ &\left(G_{11}\Psi\right)\left(G_{11}\Psi\right)^* \preceq \Gamma \end{aligned} \quad (11)$$

using the fact that $\Phi^{\mathsf{L}}\Psi^* = \Phi^{\mathsf{L}}\Psi = \Phi^{\mathsf{L}} - \Phi^{\mathsf{L}}\Phi\Phi^{\mathsf{L}} = \mathbf{0}$. Since G_{21} was assumed to have full row rank, $\Phi^*\Phi$ is a full rank square matrix and $\left(\Phi^*\Phi\right)^{\mathsf{L}} = \left(\Phi^*\Phi\right)^{-1}$. Using the Schur complement lemma on (11) results in

$$\begin{bmatrix} \Gamma - \Lambda & \left(G_{11}\Phi + G_{12}X\right) \\ \star & \Phi^*\Phi \end{bmatrix} \succeq \mathbf{0} \quad (12)$$

where $\Lambda = \left(G_{11}\Psi\right)\left(G_{11}\Psi\right)^*$. A lower-bound of $\Phi^*\Phi$ can be obtained by developing $(\Phi-\Phi_c)^*(\Phi-\Phi_c)\succeq\mathbf{0}$, for any arbitrary Φ_c as $\Phi^*\Phi \succeq \Phi^*\Phi_c + \Phi_c^*\Phi - \Phi_c^*\Phi_c$. The choice of Φ_c is an important factor in guaranteeing closed-loop stability, and will be discussed in Section 3.3.

Subject to closed-loop stability, the synthesis problem can be written as the following convex optimization problem:

$$\begin{aligned} &\min_{X\in\mathscr{X},\,Y\in\mathscr{Y},\,\Gamma}\ \gamma \\ &\text{subject to} \\ &\begin{bmatrix} \Gamma-\Lambda & \left(G_{11}\Phi + G_{12}X\right) \\ \star & \Phi^*\Phi_c + \Phi_c^*\Phi - \Phi_c^*\Phi_c \end{bmatrix}(j\omega) \succeq \mathbf{0}, \forall\omega\in\Omega \end{aligned} \quad (13)$$

3.2 Left factorization of the controller

It is assumed that G_{12} has full column rank and the controller $K = Y^{-1}X$ is left-factorized. In this case, the following equivalent problem is defined:

$$\begin{aligned} &\min_{K\in\mathscr{K},\,\Gamma}\ \gamma \\ &\text{subject to}: K \text{ stabilizes the closed-loop} \\ &\qquad T_{zw}^*(j\omega)T_{zw}(j\omega) \preceq \Gamma(j\omega), \quad \forall\omega\in\Omega \end{aligned} \tag{14}$$

Then, considering $K(I - G_{22}K)^{-1} = (I - KG_{22})^{-1}K$, the transfer function T_{zw} can be rewritten as

$$\begin{aligned} T_{zw} &= G_{11} + G_{12}\left(I - KG_{22}\right)^{-1}KG_{21} \\ &= G_{11} + G_{12}\left(Y - XG_{22}\right)^{-1}XG_{21} \end{aligned} \tag{15}$$

In contrast to Section 3.1, here G_{12} has full column rank and its left inverse exists. Define, $\Phi = \left(Y - XG_{22}\right)G_{12}^{\mathsf{L}}$, which has full row rank and therefore its right inverse is given by $\Phi^{\mathsf{R}} = G_{12}\left(Y - XG_{22}\right)^{-1}$. The closed-loop transfer function can be rewritten as

$$\begin{aligned} T_{zw} &= G_{11} + \Phi^{\mathsf{R}}XG_{21} = (\Phi^{\mathsf{R}}\Phi + \Psi)G_{11} + \Phi^{\mathsf{R}}XG_{21} \\ &= \Phi^{\mathsf{R}}\left(\Phi G_{11} + XG_{21}\right) + \Psi G_{11} \end{aligned} \tag{16}$$

where $\Psi = I - \Phi^{\mathsf{R}}\Phi = I - G_{12}G_{12}^{\mathsf{L}}$. The inequality in (14) can then be reformulated as,

$$\begin{aligned} T_{zw}^*T_{zw} = &\left(\Phi G_{11} + XG_{21}\right)^*\left(\Phi\Phi^*\right)^{\mathsf{R}}\left(\Phi G_{11} + XG_{21}\right) \\ &+(\Psi G_{11})^*(\Psi G_{11}) \preceq \Gamma \end{aligned} \tag{17}$$

using the fact that $\Psi^*\Phi^{\mathsf{R}} = \Psi\Phi^{\mathsf{R}} = \Phi^{\mathsf{R}} - \Phi^{\mathsf{R}}\Phi\Phi^{\mathsf{R}} = \mathbf{0}$. Since G_{12} was assumed to have full column rank, $\Phi\Phi^*$ is a full rank square matrix and $\left(\Phi\Phi^*\right)^{\mathsf{R}} = \left(\Phi\Phi^*\right)^{-1}$. Using the Schur complement lemma on (17),

$$\begin{bmatrix} \Gamma - \Lambda & \left(\Phi G_{11} + XG_{21}\right)^* \\ \star & \Phi\Phi^* \end{bmatrix} \succeq \mathbf{0} \tag{18}$$

where $\Lambda = (\Psi G_{11})^*(\Psi G_{11})$. Similar to Section 3.1, a lower bound on the quadratic term $\Phi\Phi^*$ can be obtained. Subject to closed-loop stability, the controller can be designed by the following convex optimization problem:

$$\begin{aligned} &\min_{X\in\mathscr{X},\,Y\in\mathscr{Y},\,\Gamma}\ \gamma \\ &\text{subject to} \\ &\begin{bmatrix} \Gamma - \Lambda & \left(\Phi G_{11} + XG_{21}\right)^* \\ \star & \Phi\Phi_c^* + \Phi_c\Phi^* - \Phi_c\Phi_c^* \end{bmatrix}(j\omega) \succeq \mathbf{0}, \forall\omega\in\Omega \end{aligned} \tag{19}$$

3.3 Stability analysis

The $\mathscr{H}_2$ or $\mathscr{H}_\infty$ norm can only be computed using the spectral formulation in (5a) or (5b) when the closed-loop system is stable. As no parametric (e.g. state-space, transfer-function, etc) model is available, the closed-loop poles cannot be computed to assess the stability. Instead, stability will be proven using the Nyquist stability criterion [27], which relates the Nyquist plot of $\det(I - G_{22}K)$ to the stability of the closed-loop system.

To proceed, we need to define a new function, wno, and its properties. Let $f(\delta) : \mathbb{C} \mapsto \mathbb{C}$ be a real rational polynomial function with no poles and zeros on a simple closed contour. Then, $\text{wno}\{f\}$ is the number of counterclockwise encirclements of $f(\delta)$ around the origin when δ traverses the contour. Two important properties of the winding number are

$$\text{wno}\{f^*\} = \text{wno}\{f^{-1}\} = -\,\text{wno}\{f\} \tag{20}$$

$$\text{wno}\{fg\} = \text{wno}\{f\} + \text{wno}\{g\} \tag{21}$$

where $g(\delta) : \mathbb{C} \mapsto \mathbb{C}$ is also a real rational polynomial function, with no poles and zeros on the contour.

Through Cauchy's argument principle, $\text{wno}\{f\}$ can be related to the number of poles and zeros of f inside the contour. This is used for the stability analysis of the closed-loop systems using the Nyquist stability criterion by defining an adequate Nyquist contour.

For continuous-time systems, the Nyquist contour is chosen as the union of the imaginary axis and a semicircle with an infinite radius enclosing the right-half plane. Since this contour is chosen clockwise oriented, $\text{wno}\{f\}$ will be equal to the number of unstable poles minus the number of unstable zeros. Note that, for a proper transfer function, the image of the semicircle with infinite radius will be constant and therefore the winding number when traversing the Nyquist contour or only the imaginary axis will be the same.

For discrete-time systems, the Nyquist contour is chosen as the counterclockwise-oriented unit circle. Therefore, the winding number is equal to the number of stable zeros minus the number of stable poles. However, if f is bi-proper, the difference in the number of stable zeros and stable poles is equal to the difference in the number of unstable poles and unstable zeros.Although the Nyquist contours are oriented differently in continuous- and discrete time, the wno in both cases is the number of unstable poles minus the number of unstable zeros. As a result, a single theorem can be used for the stability analysis of continuous- and discrete-time systems.

Theorem 1 *Given the frequency response $G(j\omega)$ of a generalized model satisfying the assumptions (A1.a) and (A2), the closed loop system with controller $K = XY^{-1}$ is stable if*

(C1) $\det(Y)$ *and* $\det(Y_c)$ *has no zeros on the stability boundary.*

(C2) $\Phi^*\Phi_c + \Phi_c^*\Phi - \Phi_c^*\Phi_c \succeq 0 \quad \forall\omega \in \Omega$, *where* Φ *is defined in* (9) *and*

$$\Phi_c = G_{21}^{\mathsf{R}} \left(Y_c - G_{22}X_c\right) \tag{22}$$

with X_c, $Y_c \in \mathscr{RH}_\infty$ *such that* $K_c = X_cY_c^{-1}$ *is a stabilizing controller.*

PROOF. The winding number of the determinant of $\Phi^*\Phi_c$ is given by

$$\text{wno}\{\det(\Phi^*\Phi_c)\} = \text{wno}\left\{\prod_{i=1}^{n}\lambda_i\right\} = \sum_{i=1}^{n}\text{wno}\{\lambda_i\} \tag{23}$$

where λ_i are the eigenvalues of $\Phi^*\Phi_c$. If the LMI in (C2) holds, and given (A1.a), $\Phi^*\Phi_c$ will be a non-Hermitian strictly positive definite matrix and all its eigenvalues have strictly positive real parts. Therefore, λ_i cannot wind around the origin and we must have $\text{wno}\{\lambda_i\} = 0$. As a result $\mathcal{W}\{\Phi^*\Phi_c\} = 0$, where for conciseness $\mathcal{W}\{\cdot\}$ is defined as $\mathcal{W}\{\cdot\} := \text{wno}\{\det(\cdot)\}$.

On the other hand, $\mathcal{W}\{\Phi^*\Phi_c\}$ can be rewritten as:

$$\begin{aligned}\underbrace{\mathcal{W}\{\Phi^*\Phi_c\}}_{=0} &= -\mathcal{W}\{Y - G_{22}X\} + \mathcal{W}\{G_{21}^{\mathsf{R}*}G_{21}^{\mathsf{R}}\} \\ &\quad +\mathcal{W}\{Y_c - G_{22}X_c\} \\ &= -\mathcal{W}\{I - G_{22}K\} - \mathcal{W}\{Y\} + \mathcal{W}\{G_{21}^{\mathsf{R}*}G_{21}^{\mathsf{R}}\} \\ &\quad +\mathcal{W}\{I - G_{22}K_c\} + \mathcal{W}\{Y_c\}\end{aligned} \tag{24}$$

By (A1.a) and (A2) and condition (C1), the Nyquist contour does not cross any zeros or poles, and the winding numbers in (24) are well-defined. From (A1.a), $G_{21}^{\mathsf{R}*}G_{21}^{\mathsf{R}}$ is a strictly positive definite matrix in all frequencies as G_{21}^{R} has full column rank. Therefore,

$$\mathcal{W}\{G_{21}^{\mathsf{R}*}G_{21}^{\mathsf{R}}\} = 0 \tag{25}$$

Since K_c is a stabilizing controller, based on the Nyquist theorem, $\mathcal{W}\{I - G_{22}K_c\} = N_{G_{22}} + N_{K_c}$, where $N_{G_{22}}$ is the number of unstable poles of G_{22}, and N_{K_c} is the number of unstable poles of K_c. Furthermore, since Y, $Y_c \in \mathscr{RH}_\infty$, $\mathcal{W}\{Y\} = -N_K$ and $\mathcal{W}\{Y_c\} = -N_{K_c}$, where N_K is the number of unstable poles of the controller K. Now using (24) and (25), we obtain

$$\begin{aligned}\mathcal{W}\{I - G_{22}K\} &= \mathcal{W}\{I - G_{22}K_c\} - \mathcal{W}\{Y\} + \mathcal{W}\{Y_c\} \\ &= N_{G_{22}} + N_K\end{aligned} \tag{26}$$

thus K stabilizes the closed-loop system. □

If the LMI (13) holds, then condition (C2) must also hold, as the last minor in (13) must also be positive. Thus, closed-loop stability is ensured with the choice Φ_c as described in (22). The following remarks are in order:

Remark 1: condition (C1) can be removed with some (infinitely small) detours on the Nyquist contour, avoiding all zeros of $\det(Y)$ and $\det(Y_c)$. However, there is no need to evaluate $\mathcal{W}\{\Phi^*\Phi_c\}$ on the new contour because its variation around the zeros of $\det(Y)$ and $\det(Y_c)$ is small and can be ignored. Similarly, (A2) can be relaxed if G_{22} has some poles on the stability boundary by some detours on the Nyquist contour, avoiding these poles. Again, there is no need to evaluate $\mathcal{W}\{\Phi^*\Phi_c\}$ on the additional detours because the contribution of $Y - G_{22}X$ and $Y_c - G_{22}X_c$ are equal (dominated by G_{22} around these poles) and therefore cancelled.

Remark 2: Note that any controller leading to unstable pole-zero cancellation in $G_{22}K$ corresponds to a point in the space of the controller parameters, which is not part of the interior of the convex set represented by the LMI in condition (C2). Because of a small variation of the controller parameters, the number of unstable poles of $G_{22}K$ changes, and the closed-loop system becomes unstable. The only possible case is to have pole-zero cancellations on the stability boundary, which are avoided by condition (C2):

- A zero of G_{22} on the stability boundary cannot be canceled as otherwise $Y - G_{22}X$ factors the same zero, Φ becomes rank deficient at the frequency of the cancelled zero, and therefore $\Phi^*\Phi_c$ cannot be strictly positive.
- If (A2) is relaxed, a pole of G_{22} on the stability boundary cannot be canceled, as otherwise there exists a vector e_1 such that $\Phi e_1 = v$ is bounded but $\Phi_c e_1 = w$ is unbounded when ω approaches the frequency of the pole on the stability boundary. This leads to a contradiction in condition (C2) as

  $$e_1^*\left(\Phi^*\Phi_c + \Phi_c^*\Phi - \Phi_c^*\Phi_c\right)e_1 = v^*w + vw^* - \|w\|^2 < 0$$

  for ω sufficiently close to the frequency of the canceled pole.

Remark 3: Building Φ_c requires an initial stabilizing controller. For stable plants, it is always possible to choose $K_c = \mathbf{0}$. For unstable systems, in a data-driven setting, it is reasonable to assume that a stabilizing controller is known since it is required for data collection. Note that other data-driven approaches also require an initial stabilizing controller [2,14], or closed-loop data [20]. In model-based approaches, such as [1,7], a stabilizing controller is also required, and is used as a starting point for the optimization routines. The difference w.r.t. other approaches is that the initial controller is used explicitly when building the constraints, not just as a starting point.

For the left factorization of the controller, the stability theorem is omitted because it is almost identical to Theorem 1, requiring (A1.b) instead of (A1.a), and $\Phi_c = (Y_c - X_cG_{22})G_{12}^{\mathsf{L}}$.

4 Controller parametrization

In this section, δ will be used to denote both the Laplace variable in the continuous-time case and the z-transform variable in the discrete-time case. In [12], the controller has the structure $K = X(\delta)Y^{-1}(\delta)$ where $X(\delta)$ and $Y(\delta)$ are defined as matrix polynomials affine in the controller parameters:

$$X(\delta) = \sum_{k=0}^{n} X_k \cdot \delta^k, \quad Y(\delta) = \sum_{k=0}^{n} Y_k \cdot \delta^k \tag{27}$$

There are two problems with this parametrization. When solving for continuous-time systems, powers of the Laplace variable $\delta^k = s^k$ evaluated on $j\omega$ will result in coefficients with large magnitudes in the constraints at high frequencies. This creates numerical problems, and most convex numerical solvers fail to give a meaningful solution. Moreover, as indicated in [2], using polynomials of degree n will generally result in controllers with much higher order in the state-space representation of multivariable systems (the order will be equal to the degree of $\det(Y)$).

In this paper, two important controller structures are investigated: (1) controllers with a fixed degree, where the degree is defined as the highest power of δ in the matrix transfer function representation of $Y(\delta)$, and (2) controllers with a fixed order, where the order is defined by the number of states in the state-space representation of the controller. Since the optimization problem is formulated directly as minimizing a function of the controller parameters, additional structure can be imposed to satisfy design requirements. It is shown how this can be used to design multivariable PID and distributed controllers.

4.1 Fixed-degree controller

To obtain an $\mathscr{RH}_\infty$ parametrization of the controller, it is possible to divide both X and Y matrix polynomials in (27) by a stable polynomial $p(\delta)$, resulting in:

$$\mathscr{X} = \left\{ X \;\middle|\; X = \sum_{k=0}^{n} X_k \cdot \frac{\delta^k}{p(\delta)} \right\} \tag{28a}$$

$$\mathscr{Y} = \left\{ Y \;\middle|\; Y = \sum_{k=0}^{n} Y_k \cdot \frac{\delta^k}{p(\delta)},\ Y_k \text{ diagonal} \right\} \tag{28b}$$

where a possible choice is $p(\delta) = (\delta - \alpha)^n$, $\alpha < 0$ for continuous-time, or $|\alpha| < 1$ for discrete-time systems. Moreover, Y is restricted to be diagonal to avoid increasing the degree of Y when inverted. Unlike the matrix polynomials, this $\mathscr{RH}_\infty$ structure leads to better numerical conditioning for continuous-time systems: the variables X_k and Y_k are not multiplied by powers of the Laplace variable $\delta^k = s^k$, which have too large magnitude on the imaginary axis. The final controller is not sensitive to the choice of α as it will be canceled when forming XY^{-1}. However, its main role is to normalize the constraints and improve the numerical accuracy of the optimization solver. Here, we give some examples of possible controller structures.

PID Controller: In CT, a multivariable PID controller $K = K_p + K_i/s + K_d\, s\,(T_f s + I)^{-1}$ can be obtained with a right factorization using (28) with $n = 2$, and $Y_0 = \mathbf{0}$ in (28b). The PID coefficients can be retrieved as follows: $T_f = Y_2 Y_1^{-1}$, $K_i = X_0 Y_1^{-1}$, $K_p = X_1 Y_1^{-1} - K_i T_f$ and $K_d = X_2 Y_1^{-1} - K_p T_f$.

Distributed Controller: Different actuators may be located physically far apart, and the various control inputs should only be computed using a subset of all measurements. Controllers for a distributed system with ℓ nodes can be designed by choosing Y_k as block diagonal matrices with $\ell \times \ell$ partitions which lead to a block diagonal Y. X is chosen such that the off-diagonal block X_k^{ij} is $\mathbf{0}$ if there is no communication of information from node j to node i. For purely decentralized controls, all off-diagonal blocks would be zero.

For example, consider a distributed control system with 3 nodes and a communication infrastructure providing bidirectional communication between nodes 1 and 2, and between nodes 2 and 3. Then the partitioned X_k and Y_k in (28) for $k \in \{0, 1, \ldots, n\}$ are given by

$$X_k = \begin{bmatrix} X_k^{11} & X_k^{12} & \mathbf{0} \\ X_k^{21} & X_k^{22} & X_k^{23} \\ \mathbf{0} & X_k^{32} & X_k^{33} \end{bmatrix} \begin{matrix} \\ \textit{Distributed} \\ \\ \textit{Local} \end{matrix} \tag{29a}$$

$$Y_k = \text{blockdiag}(Y_k^{11}, Y_k^{22}, Y_k^{33}) \tag{29b}$$

where blockdiag$(\cdot)$ is the matrix formed by diagonally stacking the input arguments, and with zeros elsewhere.

4.2 Fixed-order controllers

For designing a state-space controller of order n with right factorization $K = XY^{-1}$, we have:

$$\mathscr{X} = \{X \mid X = C_1(\delta I - A)^{-1}B + D_1\} \tag{30a}$$

$$\mathscr{Y} = \{Y \mid Y = C_2(\delta I - A)^{-1}B + D_2\} \tag{30b}$$

The optimization variables are $C_1 \in \mathbb{R}^{n_u \times n}$, $C_2 \in \mathbb{R}^{n_y \times n}$, $D_1 \in \mathbb{R}^{n_u \times n_y}$, and $D_2 \in \mathbb{R}^{n_y \times n_y}$, which leads to affine parametrization of X and Y. $A \in \mathbb{R}^{n \times n}$ and $B \in \mathbb{R}^{n \times n_y}$ are fixed and can be freely chosen, provided that A is stable, the pair (A, B) is controllable, with B having full column rank. A minimal realization of $K = XY^{-1}$ is given by

$$K = \left[\begin{array}{c|c} A - BD_2^{-1}C_2 & BD_2^{-1} \\ \hline C_1 - D_1 D_2^{-1} C_2 & D_1 D_2^{-1} \end{array}\right] \tag{31}$$

If a left factorization $K = Y^{-1}X$ is required, we have:

$$\mathscr{X} = \{X \mid X = C(\delta I - A)^{-1}B_1 + D_1\} \tag{32a}$$
$$\mathscr{Y} = \{Y \mid Y = C(\delta I - A)^{-1}B_2 + D_2\} \tag{32b}$$

where $B_1 \in \mathbb{R}^{n\times n_y}$, $B_2 \in \mathbb{R}^{n\times n_u}$, $D_1 \in \mathbb{R}^{n_u\times n_y}$, and $D_2 \in \mathbb{R}^{n_u\times n_u}$ are optimization variables, and $A \in \mathbb{R}^{n\times n}$, and $C \in \mathbb{R}^{n_u\times n}$ are constants that can be freely chosen, with the only requirement that A is stable, the pair (A, C) is observable and C full row rank. A minimal realization of $K = Y^{-1}X$ is given by

$$K = \left[\begin{array}{c|c} A - B_2D_2^{-1}C & B_1 - B_2D_2^{-1}D_1 \\ \hline D_2^{-1}C & D_2^{-1}D_1 \end{array}\right] \tag{33}$$

and has order n, irrespective of the values of the optimization variables $\{B_1, B_2, D_1, D_2\}$. Similar to the fixed-degree, additional structure can be imposed in fixed-order controllers.

Distributed Controller: For the distributed control systems with ℓ nodes, a distributed state-space controller with left factorization (LF) can be designed by choosing $\{A,\ B_2,\ C,\ D_2\}$ as block diagonal matrices with $\ell \times \ell$ partitions which lead to a block diagonal Y. On the other hand, $\{B_1,\ D_1\}$ are chosen such that B_1^{ij} and D_1^{ij} are $\mathbf{0}$ if controller for node i has no information from node j. For the decentralized controller, B_1 and D_1 would also end up being block-diagonal matrices. Similarly, for RF, $\{A, B, C_2, D_2\}$ should be block diagonal, and the off-diagonal blocks ij of $\{C_1, D_1\}$ should be zero when there is no communication link from node j to i. For the same example at the end of Section 4.1, the controller structure in LF representation can be obtained by adding constraints on A, B_1, B_2, C, D_1 and D_2 in (32):

$$A = \text{blockdiag}(A^{11}, A^{22}, A^{33}) \tag{34a}$$
$$C = \text{blockdiag}(C^{11}, C^{22}, C^{33}) \tag{34b}$$
$$B_1 = \begin{bmatrix} \boxed{B_1^{11}} & \boxed{B_1^{12}} & \mathbf{0} \\ \boxed{B_1^{21}} & \boxed{B_1^{22}} & \boxed{B_1^{23}} \\ \mathbf{0} & \boxed{B_1^{32}} & \boxed{B_1^{33}} \end{bmatrix} \begin{matrix} \\ \textit{Distributed} \\ \textit{Local} \end{matrix} \tag{34c}$$
$$D_1 = \begin{bmatrix} \boxed{D_1^{11}} & \boxed{D_1^{12}} & \mathbf{0} \\ \boxed{D_1^{21}} & \boxed{D_1^{22}} & \boxed{D_1^{23}} \\ \mathbf{0} & \boxed{D_1^{32}} & \boxed{D_1^{33}} \end{bmatrix} \begin{matrix} \\ \textit{Distributed} \\ \textit{Local} \end{matrix} \tag{34d}$$
$$B_2 = \text{blockdiag}(B_2^{11}, B_2^{22}, B_2^{33}) \tag{34e}$$
$$D_2 = \text{blockdiag}(D_2^{11}, D_2^{22}, D_2^{33}) \tag{34f}$$

5 Implementation remarks

Frequency sampling: The optimization problems presented in this paper are formulated as frequency domain inequalities and correspond to solving a convex semi-infinite program (SIP). A common approach to solve such SIP is to sample the infinite number of constraints for all points in Ω at a reasonably large finite set of frequencies $\Omega_N = \{\omega_1, \ldots, \omega_N\} \subset \Omega$. Then $\Gamma(j\omega)$ can be replaced by a hermitian matrix variable Γ_k at the corresponding frequency ω_k. The integral in (7) can be approximated using a numerical integration scheme like the trapezoidal rule. Since all constraints are applied on Hermitian matrices, constraints will also be satisfied for all negative frequencies. The formulated optimization problems are convex, and large values N can be handled by numerical solvers.

Iterative procedure: To ensure a solution to (13) or (19), the existence of the controller parameters such that $X = X_c$ and $Y = Y_c$ should be guaranteed. If this holds, a solution always exists, namely the initial controller. The controller obtained after solving (13) or (19) will depend on the choice of K_c, the resulting controller can be of poor performance. It is proposed to solve the problem iteratively, using the optimal controller as the initial controller for the next iteration. The objective is non-increasing, as the initial controller is always a feasible solution and the problem is convex in the optimization parameters. The final controller will converge to a local minimum or saddle point of (6).

Remark: For the fixed-order controllers, it is useful, after each iteration, to compute a balanced realization [15] of the initial controller, then compute the coprime factorization [28] to obtain X_c and Y_c for the next iteration. This will also avoid convergence to a factorization where D_2 is singular, as D_2 is normalized at each iteration.

Implementation Algorithm: As a token implementation example, it is desired to solve a mixed $\mathscr{H}_2/\mathscr{H}_\infty$ synthesis problem

$$\min_{K\in\mathscr{K}} \ \gamma$$
$$\|\mathscr{F}_l(G, K)\|_2 \le \gamma, \quad \left\|\mathscr{F}_l(\overline{G}, K)\right\|_\infty \le 1 \tag{35}$$

with a fixed-order controller, using the formulation proposed in Section 3.1. Given the two generalized plants G, $\overline{G}$, an initial stabilizing controller $K_c = X_cY_c^{-1}$ and the frequency grid Ω_N, the mixed norm problem can be implemented as described in Algorithm 1, where the variables $\overline{\Phi}$, $\overline{\Phi}_c$ and $\overline{\Lambda}$ are defined using $\overline{G}(j\omega_k)$.

6 Simulation Results and Comparisons

In this section, benchmarks are employed to compare the performance of our proposed approach with other structured controller synthesis methods that utilize parametric models. However, it is important to note that our approach is not limited to parametric models. It can also be applied when the frequency response function is obtained in a data-driven manner.

Algorithm 1 Example $\mathscr{H}_2/\mathscr{H}_\infty$ mixed synthesis problem implementation with fixed-order controller

1: From input/output data, compute $P(e^{j\omega})$, e.g., using (3). Construct $G, \overline{G}$, corresponding to the desired objectives, e.g., (40) for $\mathscr{H}_2$ closed-loop model-matching with an additional $\mathscr{H}_\infty$ constraint.
2: If the system is stable, use $X_c = \mathbf{0}, Y_c = I$. If the system is unstable, factorize the stabilizing controller used for data acquisition as $K_c = X_c Y_c^{-1}$.
3: Solve the sampled-frequency version of the optimization problem

$$\min_{X\in\mathscr{X},\, Y\in\mathscr{Y}} \sum_{k=2}^{N} (\omega_k - \omega_{k-1}) \cdot \operatorname{trace}(\Gamma_k)$$
subject to
$$\begin{bmatrix} \Gamma_k - \Lambda & (G_{11}\Phi + G_{12}X) \\ \star & \Phi^*\Phi_c + \Phi_c^*\Phi - \Phi_c^*\Phi_c \end{bmatrix}(j\omega_k) \succeq \mathbf{0} \quad (36)$$
$$\begin{bmatrix} I - \overline{\Lambda} & \left(\overline{G}_{11}\overline{\Phi} + \overline{G}_{12}X\right) \\ \star & \overline{\Phi}^*\overline{\Phi}_c + \overline{\Phi}_c^*\overline{\Phi} - \overline{\Phi}_c^*\overline{\Phi}_c \end{bmatrix}(j\omega_k) \succeq \mathbf{0}$$
$$\forall \omega_k \in \{\omega_1, \ldots, \omega_N\}$$

4: Compute a minimal realization of $K = XY^{-1}$. If K is a local minimum of (35) stop, otherwise define K_c as a balanced realization of K, factorize $K_c = X_c Y_c^{-1}$ and go to step 3.

6.1 Comparison with non-smooth optimization

The problem of interest is a mixed-sensitivity problem:

$$\min_{K\in\mathscr{K}} \left\| \begin{bmatrix} W_1(I+PK)^{-1} \\ W_3K(I+PK)^{-1} \end{bmatrix} \right\|_\infty \quad (37)$$

where $W_1 = (s+3)/(3s+0.3)$ and $W_2 = (10s+2)/(s+40)$. The process model and corresponding generalized system are given by:

$$P = \begin{bmatrix} \frac{1}{s+1} & \frac{0.2}{s+3} & \frac{0.3}{s+0.5} \\ \frac{0.1}{s+2} & \frac{1}{s+1} & \frac{1}{s+1} \\ \frac{0.1}{s+0.5} & \frac{0.5}{s+2} & \frac{1}{s+1} \end{bmatrix}, \quad G = \left[\begin{array}{c|c} W_1 I & -W_1 P \\ \mathbf{0} & W_2 I \\ \hdashline I & -P \end{array}\right] \quad (38)$$

The control objective is to minimize $\|\mathscr{F}_l(G,K)\|_\infty$. This problem is studied in [2] and [12]. In [12], the controller has a polynomial structure as given in (27), and could not be fairly compared with the non-smooth optimization algorithm in [2]. Here, using state-space parameterization, low-order state-space controllers can be designed, and the algorithm is numerically improved, leading to the results in Table 1. The initial stabilizing controller $K_c = \mathbf{0}$ is used as the process model is stable. The problem is implemented using Yalmip [17], and solved at 400 logarithmically spaced frequencies in $[10^{-4}, 10^4]$ using the convex solver *mosek* (`http://www.mosek.com`). The results show the improvement over [12].

Table 1
Fixed-order comparison.

Controller order	Method		
	[12]	[2]	Proposed
1	na	6.27	6.27
2	na	5.13	5.13
3	1.52	1.43	1.43
4	na	1.22	1.22
5	na	1.22	1.22
6	1.25	1.21	1.21

6.2 Comparison with `HIFOO` and `SYSTUNE`

The proposed approach is now compared with model-based fixed-structure controller design approaches called `HIFOO` [7] and `SYSTUNE` in `MATLAB` [3] (which implements `HINFSTRUCT` [1] in the $\mathscr{H}_\infty$ case). The objective of the presented approach is not to replace such methods, but rather propose an efficient alternative when specialized solvers and parametric models are not available, but only the frequency domain data. The examples are taken from the COMPl$_e$ib library [16]. This library regroups a collection of control-relevant problems arising from the engineering literature or real-life problems and is made available to test and compare different algorithms. Importantly, many of the examples could not be solved using [12], as most of the provided examples cannot be cast as a mixed-sensitivity problem. An effort is made to select at least one system from all categories. In particular, the systems chosen have no feed-through, such that the $\mathscr{H}_2$ norm can be finite, and taken in ascending order.

Similar to the proposed method, `HIFOO` and `SYSTUNE` require an initial stabilizing controller. For stable systems, the controller $K_c = \mathbf{0}$ is used. For unstable systems, the same initialization method as employed by `HIFOO` is used. A frequency grid is chosen as 400 logarithmically spaced points between $[10^{-4}, 10^4]$ for all $\mathscr{H}_\infty$ examples and 100 logarithmically spaced points for the $\mathscr{H}_2$ examples. The optimization time can be significantly reduced using a better selection of the frequencies, e.g. as proposed in [2]. The class of controllers $\mathscr{K}$ is chosen as 2^{nd} order controllers. The iterative procedure described in Section 5 is used to converge to a local minimum, where at each iteration, first a balanced realization is computed, then an appropriate controller factorization to obtain X_c, Y_c. The iterative approach is stopped when the objective decreases less than 10^{-4} between two consecutive iterations. The final objective value can be found in Table 2 and in Table 3 for the $\mathscr{H}_\infty$ and $\mathscr{H}_2$ case, respectively. The

Table 2
$\mathscr{H}_\infty$ performance on some COMPl$_e$ib problems. Solve time: time spent in the convex solver (in seconds).

Problem	Second-order Controller			Full order optimal	Solve time (sec.)
	Proposed	HIFOO	SYSTUNE		
AC1	0.0000	0.0000	0.0000	0.0000	1.29
AC2	0.1115	0.1115	0.1115	0.1115	4.15
AC3	2.9683	3.2972	3.1164	2.9675	12.0
AC5	662.41	667.74	664.06	657.10	19.1
HE1	0.0740	0.0930	0.0897	0.0736	1.88
JE1	4.2970	22.163	4.1101	3.8537	118
REA1	0.8617	0.8617	0.8617	0.8617	2.92
DIS1	4.1597	4.1650	4.1602	4.1593	7.55
DIS2	0.9476	0.9571	0.9531	0.9474	4.49
TG1	3.4652	3.4653	3.4652	3.4652	32.9
AGS	8.1732	8.1732	8.1732	8.1732	2.21
WEC1	3.6363	3.6363	3.6363	3.6363	3.96
WEC2	3.5981	3.6103	3.5981	3.5981	3.84
HF1	0.4472	0.4472	0.4472	0.4472	0.20
BDT1	0.2663	0.2662	0.2662	0.2662	0.75
MFP	4.3314	4.3862	4.8393	4.1866	9.29
PSM	0.9202	0.9202	0.9202	0.9202	0.69

results of optimal full-order controllers are also reported, showing that the local optimal solutions achieved by reduced-order controllers are very close to the full-order solution. The proposed method achieves equivalent performance to model-based methods but requires longer optimization times. The proposed approach is not intended to replace the synthesis methods when a parametric model is available, but is useful when only the frequency response is given.

6.3 Impact of initial controller

As mentioned in Section 5, the choice of the initial controller is essential for solving the optimization problem. When following the iterative procedure, it is shown through an example, the final achieved performance is not sensitive to the choice of the initial controller. The example AC4 from COMPl$_e$ib is considered, and the corresponding $\mathscr{H}_\infty$ problem is solved. As reported in [7], HIFOO reliably finds an optimal controller of order 0 (with objective value 0.935), but it sometimes fails to find the optimal controller for orders 1 and 2 (both achieving an objective value of 0.557). For each controller order, 100 different random initial controllers have been chosen. Using the same heuristic as they employ to find a stabilizing initial controller, the proposed approach empirically converges every time to a local minimum with

Table 3
$\mathscr{H}_2$ performance on some COMPl$_e$ib problems. Solve time: time spent in the convex solver (in seconds).

Problem	Second-order Controller			Full order optimal	Solve time (sec.)
	Proposed	HIFOO	SYSTUNE		
AC1	0.0000	0.0000	0.0000	0.0000	0.32
AC2	0.0500	0.0491	0.0492	0.0491	5.22
AC3	4.2721	4.2717	4.2717	4.2717	8.15
AC5	1342.0	1342.1	1342.1	1339.7	6.74
HE1	0.0904	0.0870	0.0876	0.0855	0.40
JE1	43.517	42.891	42.901	42.860	144
REA1	1.5041	1.5041	1.5041	1.5041	2.67
DIS1	2.6603	2.6601	2.6600	2.6600	1.24
DIS2	1.4044	1.4016	1.4016	1.4016	0.91
TG1	9.7945	9.7060	9.7060	9.1817	65.3
AGS	6.7274	6.6587	6.6580	6.6303	11.4
WEC1	5.7267	5.7175	5.7609	5.6931	87.0
WEC2	5.8987	5.8920	5.8863	5.8671	184
HF1	0.0581	0.0581	0.0581	0.0580	0.11
BDT1	0.0096	0.0100	0.0098	0.0094	0.47
MFP	3.9168	3.9148	3.9148	3.9148	6.12
PSM	1.4557	1.4425	1.4355	1.4191	2.06

objective value 0.935 for order 0, and 0.557 for order 1 or 2, as can be seen in Figure 2.

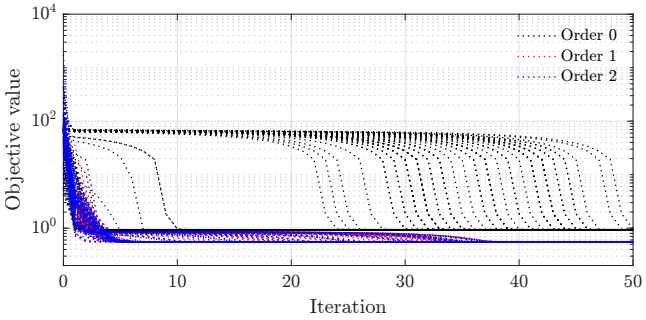

Fig. 2. Objective achieved for different controller orders.

7 Experimental Results

In this section, real data from a laboratory setup is collected and used to design a discrete-time controller sampled at $T_s = 0.002$ s. It is shown how the proposed approach can deal with multimodel uncertainty, measurement noise, and mixed $\mathscr{H}_2/\mathscr{H}_\infty$ synthesis. This example focuses on the velocity control of a DC motor with a flexible element attached on top. Different weights can be attached to the flexible element, at different positions, resulting in multimodel uncertainty.

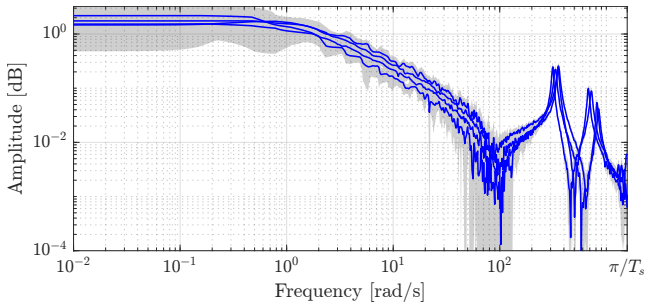

Fig. 3. Plant magnitude frequency response and variance (two standard deviations).

The frequency function is obtained from input-output data at 4 positions of the weights, leading to different models $P(e^{j\omega}) = \{P_1(e^{j\omega}), \ldots, P_4(e^{j\omega})\}$. For every model P_i, a multiplicative uncertainty filter W_i is obtained, corresponding to two times the standard deviation of the FRF estimate. Both are obtained using spectral analysis, see Chapter 2 in [23]. The FRF of P and its confidence interval are shown in Figure 3.

The objective is to obtain a closed-loop similar to a given reference closed-loop model $\mathscr{T}_r$ obtained by squaring a first-order low-pass filter with DC-gain 1 and bandwidth 11.5 rad/s. The problem is formulated as $\mathscr{H}_2$ closed-loop matching, minimizing the worst performance over the different models:

$$\min_{K} \max_{i=1,\ldots,4} \|F(\omega) \cdot (\mathscr{T}_r - \mathscr{T}_i)\|_2 \tag{39}$$

where $F(\omega) = 1 + 1/\omega$ is a weighting filter and $\mathscr{T}_i$ is the closed-loop transfer function using the model P_i. Additionally, the closed-loop system must satisfy a robust stability condition: $\|W_i \mathscr{T}_i\|_\infty \leq 1$ corresponding to multiplicative noise-originated uncertainty, which can be formulated as $\|\mathscr{F}_l(\overline{G}_i, K)\|_\infty \leq 1 \quad i = 1, \ldots, 4$. The generalized systems are

$$G_i = \left[\begin{array}{c|c} F \cdot \mathscr{T}_r & -F \cdot P_i \\ \hline 1 & -P_i \end{array}\right], \quad \overline{G}_i = \left[\begin{array}{c|c} 0 & W_i P_i \\ \hline 1 & -P_i \end{array}\right] \tag{40}$$

Finally, a discrete-time controller $K = X(z)Y^{-1}(z)$ of order 8 is designed using (30) parametrization. To ensure integral action in the controller, the constraint $Y(z=1) = 0$ is added to the problem. The optimization problem to solve is therefore

$$\begin{aligned} &\min_{X \in \mathscr{X},\, Y \in \mathscr{Y}} \max_{i=1,\ldots,4} \gamma_i \\ &\left\|\mathscr{F}_l(G_i, XY^{-1})\right\|_2 \leq \gamma_i, \quad i = 1, \ldots, 4 \\ &\left\|\mathscr{F}_l(\overline{G}_i, XY^{-1})\right\|_\infty \leq 1, \quad i = 1, \ldots, 4 \\ &Y(z=1) = 0 \end{aligned} \tag{41}$$

The problem is sampled at 500 logarithmically spaced $\omega \in [10^{-2}, \pi/T_s]$, with both LFTs implemented as described in Algorithm 1. The closed-loop tracking of a square waveform reference, obtained after tuning, is shown in Figure 4, along with the desired output of the reference model $\mathscr{T}_r$. As can be seen, the different closed-loop using different loads follow the reference model.

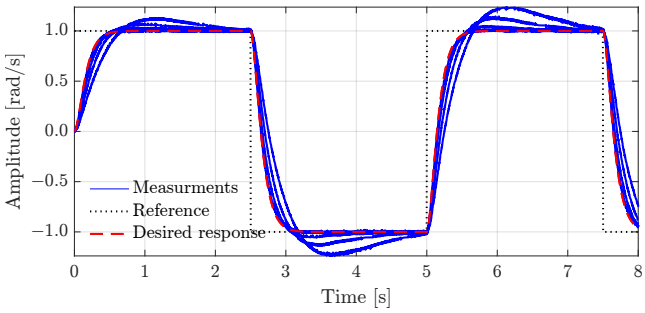

Fig. 4. Closed-loop tracking at different operating points.

8 Conclusion

This paper presents a novel synthesis method for designing structured $\mathscr{H}_\infty$ or $\mathscr{H}_2$ controllers using frequency-domain data of a generalized plant model. The control problem is formulated as a convex-concave optimization problem, leveraging an appropriate controller parametrization. By utilizing an initial stabilizing controller and frequency sampling, the problem is transformed into a tractable SDP and efficiently solved. Compared to [12], the proposed method offers several advantages, including applicability to generalized plants, the ability to design fixed-order state-space controllers, and improved numerical precision. Despite utilizing only frequency response data, the proposed method yields comparable results to state-of-the-art model-based approaches and global optimal solutions.

References

[1] P. Apkarian and D. Noll. Nonsmooth $\mathscr{H}_\infty$ synthesis. *IEEE Transactions on Automatic Control*, 51(1):71–86, 2006.

[2] P. Apkarian and D. Noll. Structured $\mathscr{H}_\infty$ control of infinite-dimensional systems. *International Journal of Robust and Nonlinear Control*, 28(9):3212–3238, 2018.

[3] P. Apkarian, D. Noll, and A. Rondepierre. Mixed $\mathscr{H}_2/\mathscr{H}_\infty$ control via nonsmooth optimization. *SIAM Journal on Control and Optimization*, 47(3):1516–1546, 2008.

[4] O. Baghernieh and R. Horowitz. Mixed $\mathscr{H}_2/\mathscr{H}_\infty$ data-driven control design for hard disk drives. In *2018 Asia-Pacific Magnetic Recording Conference*, pages 1–3, 2018.

[5] T. Bloemers, T. Oomen, and R. Toth. Frequency Response Data-Driven LPV Controller Synthesis for MIMO Systems. *IEEE Control Syst. Lett.*, 6:2264–2269, 2022.

[6] S. Boyd, M. Hast, and K. J. Åström. MIMO PID tuning via iterated LMI restriction. *Int. J. Robust Nonlinear Control*, 26(8):1718–1731, May 2016.

[7] J. V. Burke, D. Henrion, A. S. Lewis, and M. L. Overton. HIFOO - A MATLAB package for fixed-order controller

design and $\mathscr{H}_\infty$ optimization. *IFAC Proceedings Volumes*, 39(9):339–344, 2006.

[8] S. Formentin, K. Van Heusden, and A. Karimi. A comparison of model-based and data-driven controller tuning. *Int. Journal of Adaptive Control and Signal Processing*, 28(10):882–897, 2014.

[9] M. Hast, K. J. Åström, B. Bernhardsson, and S. Boyd. PID design by convex-concave optimization. In *European Control Conference*, pages 4460–4465, Zurich, Switzerland, 2013.

[10] C. Kammer, A. P. Nievergelt, G. Fantner, and A. Karimi. Data-driven controller design for atomic-force microscopy. *IFAC-PapersOnLine*, 50(1):10437–10442, 2017.

[11] A. Karimi and G. Galdos. Fixed-order $\mathscr{H}_\infty$ controller design for nonparametric models by convex optimization. *Automatica*, 46(8):1388–1394, 2010.

[12] A. Karimi and C. Kammer. A data-driven approach to robust control of multivariable systems by convex optimization. *Automatica*, 85:227–233, Nov. 2017.

[13] A. Karimi, A. Nicoletti, and Y. Zhu. Robust $\mathscr{H}_\infty$ controller design using frequency-domain data via convex optimization. *Int. J. Robust Nonlinear Control*, 28(12):3766–3783, 2018.

[14] L. H. Keel and S. P. Bhattacharyya. Controller Synthesis Free of Analytical Models: Three Term Controllers. *IEEE Trans. Automat. Contr.*, 53(6):1353–1369, July 2008.

[15] A. Laub, M. Heath, C. Paige, and R. Ward. Computation of system balancing transformations and other applications of simultaneous diagonalization algorithms. *IEEE Transactions on Automatic Control*, 32(2):115–122, 1987.

[16] F. Leibfritz. COMPl$_e$ib: Constrained matrix optimization problem library. 2006. Online at `http://www.compleib.de`.

[17] J. Löfberg. YALMIP: A toolbox for modeling and optimization in MATLAB. In *2004 International conference on robotics and automation*, pages 284–289, 2004.

[18] S. S. Madani, C. Kammer, and A. Karimi. Data-driven distributed combined primary and secondary control in microgrids. *IEEE Transactions on Control Systems Technology*, 29(3):1340–1347, 2020.

[19] P. Mercader, K. J. Astrom, A. Banos, and T. Hagglund. Robust PID Design Based on QFT and Convex–Concave Optimization. *IEEE Transactions on Control Systems Technology*, 25(2):441–452, 2017.

[20] A. Nicoletti, M. Martino, and A. Karimi. A robust data-driven controller design methodology with applications to particle accelerator power converters. *IEEE Transactions on Control Systems Technology*, 27(2):814–821, 2018.

[21] A. Nicoletti, M. Martino, and A. Karimi. A data-driven approach to model-reference control with applications to particle accelerator power converters. *Control Engineering Practice*, 83:11–20, 2019.

[22] N. Nikooienejad and S. O. R. Moheimani. Frequency domain-based integral resonant control design for a MEMS nanopositioner. In *IEEE Conference on Control Technology and Applications*, pages 874–879, 2021.

[23] R. Pintelon and J. Schoukens. *System identification: a frequency domain approach*. John Wiley & Sons, 2012.

[24] M. Saeki. Data-driven loop-shaping design of PID controllers for stable plants. *International Journal of Adaptive Control and Signal Processing*, 28(12):1325–1340, 2014.

[25] M. Saeki, M. Ogawa, and N. Wada. Low-order $\mathscr{H}_\infty$ controller design on the frequency domain by partial optimization. *International Journal of Robust and Nonlinear Control*, 20(3):323–333, 2010.

[26] P. Shah and R. Horowitz. Data-driven feedforward control design and input shaping techniques for multi actuator drives. *ASME Letters in Dynamic Systems and Control*, 1(3), 2021.

[27] S. Skogestad and I. Postlethwaite. *Multivariable feedback control: analysis and design*. john Wiley & sons, 2005.

[28] K. Zhou, J. C. Doyle, and K. Glover. *Robust and Optimal Control*. Prentice Hall, New Jersey, USA, 1996.

Philippe Schuchert received his B.Sc. and M.Sc. degrees in mechanical engineering from École Polytechnique Fédérale de Lausanne (EPFL), Lausanne, Switzerland, in 2016 and 2018, respectively. He is currently pursuing his Ph.D. degree in the doctoral program for *Robotics, Control, and Intelligent Systems* at the data-driven modeling and control group of the Automatic Control Laboratory at EPFL. From 2018 to 2020, he was a Research Assistant with the Automatic Control Laboratory. His research interest includes data-driven $\mathscr{H}_2$ and $\mathscr{H}_\infty$ control with application to high-precision mechatronic systems.

Vaibhav Gupta holds a bachelor's degree in mechanical engineering from IIT Delhi, India (2017) and a master's in robotics from École Polytechnique Fédérale de Lausanne (EPFL), Switzerland (2021). Currently, he is pursuing a Ph.D. in Robotics, Control, and Intelligent Systems as a part of Data-Driven Modelling and Control Group in the Automatic Control Laboratory at EPFL. Before pursuing his master's degree, he gained experience in the automobile industry. His current research is centered on developing robust data-driven control methods with practical applicability across various domains.

Alireza Karimi received the Ph.D. degree from the Polytechnic National Institute of Grenoble in France, in 1997. He was an Assistant Professor with the Department of Electrical Engineering, Sharif University of Technology in Tehran, Iran, from 1998 to 2000. He then joined the École Polytechnique Fédérale de Lausanne (EPFL), Switzerland, where he is currently a Professor of automatic control with the Mechanical Engineering Institute. He is also the leader of the Data-Driven Modeling and Control Group situated at the Automatic Control Laboratory. His research focuses on data-driven controller design for power grids and mechatronic systems. Prof. Karimi contributed as an Associate Editor for the European Journal of Control between 2004 and 2013. Additionally, he has been an active member of the IEEE Control Systems Society's Conference Editorial Board since 2018.